

PROPERTIES OF  $\gamma$ -DECAYING ISOMERS IN THE  $^{100}\text{Sn}$   
REGION REVISITED\*

G. HAEFNER<sup>a</sup>, K. MOSCHNER<sup>a</sup>, A. BLAZHEV<sup>a</sup>, P. BOUTACHKOV<sup>b</sup>  
P.J. DAVIES<sup>c</sup>, R. WADSWORTH<sup>c</sup>, F. AMEIL<sup>b</sup>, H. BABA<sup>d</sup>, T. BÄCKE<sup>e</sup>  
M. DEWALD<sup>a</sup>, P. DOORNENBAL<sup>d</sup>, T. FAESTERMANN<sup>f</sup>  
A. GENGELBACH<sup>g</sup>, J. GERL<sup>b</sup>, R. GERNHÄUSER<sup>f</sup>, S. GO<sup>h</sup>, M. GÓRSKA<sup>b</sup>  
H. GRAWE<sup>b</sup>, E. GREGOR<sup>i</sup>, H. HOTAKA<sup>j</sup>, T. ISOBE<sup>d</sup>, D.G. JENKINS<sup>c</sup>  
J. JOLIE<sup>a</sup>, H.S. JUNG<sup>k</sup>, I. KOJOUHAROV<sup>b</sup>, N. KURZ<sup>b</sup>, M. LEWITOWICZ<sup>l</sup>  
G. LORUSSO<sup>d</sup>, E. MERCHAN<sup>i</sup>, F. NAQVI<sup>m</sup>, H. NISHIBATA<sup>n</sup>  
D. NISHIMURA<sup>o</sup>, S. NISHIMURA<sup>d</sup>, N. PIETRALLA<sup>i</sup>, H. SCHAFFNER<sup>b</sup>  
P.-A. SÖDERSTRÖM<sup>d</sup>, K. STEIGER<sup>f</sup>, T. SUMIKAMA<sup>p</sup>, J. TAPROGGE<sup>q,r</sup>  
P. THÖLE<sup>a</sup>, H. WATANABE<sup>s</sup>, N. WARR<sup>a</sup>, V. WERNER<sup>i,m</sup>, Z.Y. XU<sup>h</sup>  
A. YAGI<sup>n</sup>, K. YOSHINAGA<sup>j</sup>, Y. ZHU<sup>j</sup>

<sup>a</sup>Institut für Kernphysik, University of Cologne, Germany

<sup>b</sup>Gesellschaft für Schwerionenforschung, Darmstadt, Germany

<sup>c</sup>Department for Physics, University of York, UK

<sup>d</sup>RIKEN Nishina Center, Wako, Japan

<sup>e</sup>Department of Physics, KTH Stockholm, Sweden

<sup>f</sup>Technische Universität München, Germany

<sup>g</sup>Physics Division, Uppsala University, Sweden

<sup>h</sup>University of Tokyo, Japan

<sup>i</sup>Technische Universität Darmstadt, Germany

<sup>j</sup>Tokyo University of Science, Japan

<sup>k</sup>Chung-Ang University, Seoul, Korea

<sup>l</sup>Grand Accélérateur Nation d'Ions Lourdes, Caen, France

<sup>m</sup>Yale University, USA

<sup>n</sup>Osaka University, Japan

<sup>o</sup>Tokyo City University, Japan

<sup>p</sup>Tohoku University, Japan

<sup>q</sup>Institute of the Structure of Matter, CSIC Madrid, Spain

<sup>r</sup>Universidad Autónoma de Madrid, Spain

<sup>s</sup>Beihang University, China

*(Received November 30, 2018)*

---

\* Presented at the Zakopane Conference on Nuclear Physics “Extremes of the Nuclear Landscape”, Zakopane, Poland, August 26–September 2, 2018.

The study of nuclei in the region around the  $N = Z$  doubly-magic nucleus  $^{100}\text{Sn}$  has been of long standing interest for the nuclear structure and nuclear astrophysics. Recently, Park *et al.* have reported on properties of  $\gamma$ -decaying isomers and isomeric ratios in the vicinity of  $^{100}\text{Sn}$ . That experiment was performed at the Radioactive Ion Beam Factory (RIBF) of the RIKEN Nishina Center in Japan as a part of the EURICA campaign. Neutron-deficient nuclei were produced in a fragmentation reaction of a  $^{124}\text{Xe}$  primary beam on a  $^9\text{Be}$  target at an energy of 345 MeV/ $A$ . Secondary ions were separated and identified in the BigRIPS fragment separator and implanted in the silicon detector array WAS3ABi. The data presented here were obtained in another experiment performed at the RIBF using the same reaction but slightly different separator settings. New results of ratios of isomeric population and half-lives of  $\gamma$ -decaying isomers populated in the experiment are presented.

DOI:10.5506/APhysPolB.50.431

## 1. Introduction

$^{100}\text{Sn}$  is the heaviest  $N = Z$  ( $= 50$ ) doubly-magic nucleus and lies close to the proton dripline. The region of  $N \sim Z$  nuclei around  $^{100}\text{Sn}$  is of great importance as a testing ground for the nuclear shell-model and effective interactions while also being strongly connected to the astrophysical rapid-proton capture process (rp-process) [1]. An extensive review on the nuclear structure phenomena and the implications for nuclear astrophysics can be found in Ref. [2] and references therein. Due to the shell structure of atomic nuclei and the residual interaction between individual nucleons, the region south-west of  $^{100}\text{Sn}$  has a high abundance of different types of isomers. Recently, Park *et al.* [3] presented results on  $\gamma$ -decaying isomers and isomeric ratios in this region. The data analysed in this work was obtained independently in a similar experiment and provides further information on  $\gamma$ -decaying isomers in that region.

## 2. Experiment and analysis

The experiment RIBF83 was conducted at the Radioactive Ion Beam Factory of the RIKEN Nishina Center within the EURICA campaign [4]. Previously, results from the RIBF83 experiment have been published in Refs. [5–7]. Neutron-deficient isotopes were produced in a fragmentation reaction of a  $^{124}\text{Xe}$  beam accelerated to 345 MeV/ $A$  on a 4 mm  $^9\text{Be}$  target. Secondary ions were separated in the first stage of BigRIPS using an aluminium wedge degrader, dipole magnets, and slits. Further separation and an event-by-event identification was achieved in the second stage of the fragment separator by the  $B\rho$ -TOF- $\Delta E$  method [8]. Figure 1 shows a  $Z$  vs.  $A/Q$  plot of the identified isotopes in the range of  $40 \leq Z \leq 50$ .

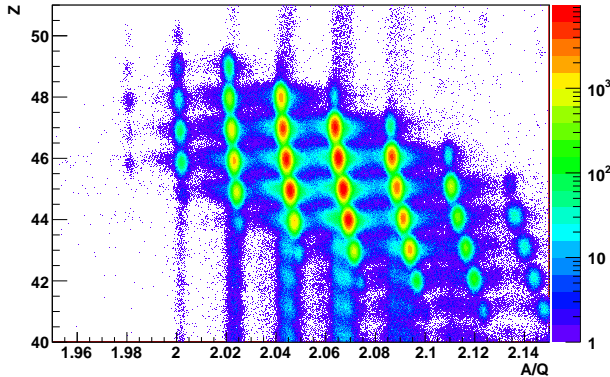


Fig. 1. Particle identification plot showing the production and identification of isotopes in this experiment.

The ions were implanted in a modified version of the Silicon IMplantation Beta Absorber (SIMBA) [9, 10] after a flight time of around 700–800 ns. The active stopper SIMBA was surrounded by the Euroball-RIKEN Cluster Array (EURICA) consisting of 84 HPGe crystals to detect the  $\gamma$  rays. During the RIBF83 experiment, 81 channels were active. Each HPGe crystal was connected with two preamplifier outputs, one of them handled in an analogue branch and the other digitally processed via digital  $\gamma$ -finder (DGF) modules. The DGF modules provide a  $\gamma$ -ray acquisition time window up to 90  $\mu\text{s}$ . Together with the flight time, it restricts the analysis of  $\gamma$ -decaying isomeric states to the half-life range of approximately  $100 \text{ ns} \leq T_{1/2} \leq 100 \mu\text{s}$ .

The half-lives were analysed with the help of selection cuts in the particle identification plot and characteristic  $\gamma$ -ray energies following the decay of isomeric states. First, an energy gate on  $\gamma$  rays belonging to the decay cascade of an isomer was applied to generate time spectra. Then, exponential decay curves modified with a constant background function were fitted with the maximum likelihood method to obtain the half-life. This value is very sensitive to the fit region which is why the fit limits were systematically varied in order to introduce a statistical uncertainty expressed by the  $1\sigma$  range.

Experimental isomeric ratios were obtained based on the approach from Ref. [11]. The formula was modified by a correction factor for prompt flash events [12] resulting in  $R_{\text{exp}} = \frac{Y}{N_{\text{imp}} f_1 f_2 f_3}$ , where  $Y$  is the absolute yield of the isomeric decay,  $N_{\text{imp}}$  the number of implanted ions and  $f_{1-3}$  factors correcting for prompt flash events, in-flight decay and finite  $\gamma$ -ray detection window, respectively.

### 3. Results on isomeric half-lives

Half-lives of 20  $\gamma$ -decaying isomers in neutron-deficient isotopes between  $Z = 40$  (Zr) and  $Z = 48$  (Cd) were remeasured [13]. As an example for the quality of the obtained data, the time spectrum and decay curve to determine the half-life of the  $8^+$  isomer in  $^{90}\text{Mo}$  is shown in Fig. 2. The preliminary value for the half-life of  $1.1(1) \mu\text{s}$  is consistent with the literature [14]. Transition probabilities were deduced from the obtained half-lives and compared to SM calculations. The calculations were performed using the code NushellX [15] in the  $\pi\nu(p_{1/2}g_{9/2})$  model space and the isospin-symmetric SLGT0PN interaction from the NushellX package. The theoretical transition strengths were calculated using two sets of effective charges (a) standard effective charges  $e_\pi = 1.5e$ ,  $e_\nu = 0.5e$  and (b) to the charges of  $e_\pi = 1.7e$ ,  $e_\nu = 1.4e$ , which were tuned to experimental values. In general, the results from the SM calculation are in a good agreement with the experimentally deduced  $B(\sigma\lambda)$ -values except for isomers in  $^{92,94}\text{Ru}$  and  $^{98}\text{Cd}$  [13].

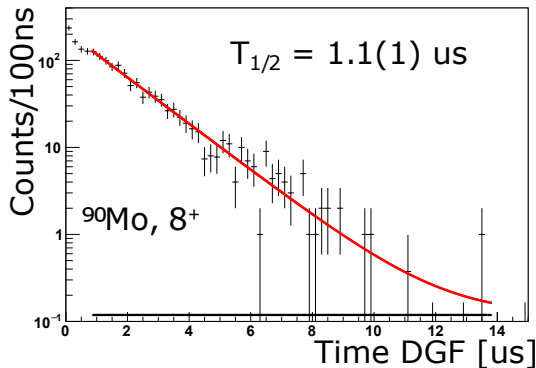


Fig. 2. Time distribution and decay curve of the  $8^+$  isomer in  $^{90}\text{Mo}$ .

Park *et al.* [3] reported on two new low-energy isomeric transitions in  $^{92}\text{Rh}$  and  $^{96}\text{Ag}$ . By constraining the DGF time window, prompt flash events are suppressed in the  $\gamma$ -ray spectrum. This reveals a transition at approximately 55 keV belonging to  $^{92}\text{Rh}$ , see Fig. 3 (a). The obtained half-life value is consistent with the result of  $0.23(6) \mu\text{s}$  from Ref. [3] supporting the  $(4^+)$  assignment for the isomer in  $^{92}\text{Rh}$  [3, 13].

The transition energy from the  $(15^+)$  isomer to the  $(13^+)$  state of  $^{96}\text{Ag}$  was measured by Park *et al.* [3] for the first time and determined to be  $43.7(2) \text{keV}$ . By choosing an appropriate time window of  $500 \text{ ns} \leq t \leq 6.5 \mu\text{s}$ , a preliminary value of  $44.1(5) \text{keV}$  for this transition could be obtained in the present work which is consistent within the error bars [13]. Figure 3 (b) shows the projected  $\gamma$ -ray energies in  $^{96}\text{Ag}$  revealing the low-energy transition and confirming the results from Ref. [3].

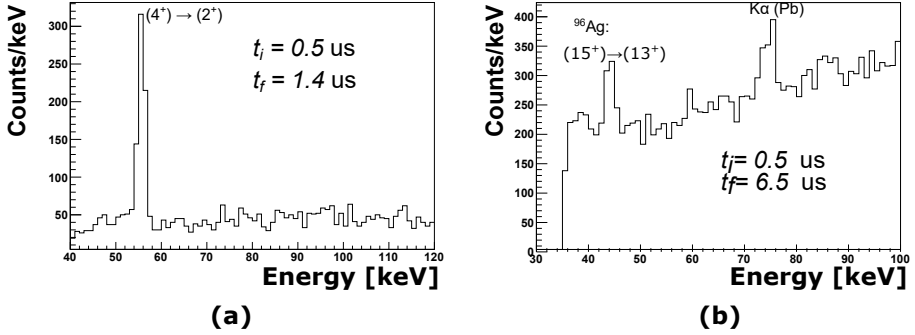


Fig. 3. Low-energy isomeric transitions in (a)  $^{92}\text{Rh}$  and (b)  $^{96}\text{Ag}$ .  $t_i$ ,  $t_f$  are initial and final  $\gamma$ -ray acquisition time set in the offline analysis.

#### 4. Results on isomeric ratios

The population of an isomeric state in a nuclear (fragmentation) reaction is described by the isomeric ratio as defined in Sec. 2 which describes the probability that an observed decay of an isomeric state originates from the initial population. In this section, the experimental isomeric ratios  $R_{\text{exp}}$  determined in this work are compared to theoretical values  $R_{\text{theor}}$ . The latter ones are calculated using the sharp cut-off model (SCM) first introduced by de Jong, Ignatyuk and Schmidt [16] which make use of the statistical abrasion–ablation model [17]. The isomeric ratio can be estimated by integrating the spin probability  $P_J$  from the isomeric spin of interest up to infinity

$$R_{\text{theor}} = \int_{J_m}^{\infty} P_J dJ = e^{-J_m(J_m+1)/2\sigma_f^2}, \quad (1)$$

where  $\sigma_f$  is the spin distribution width of the final fragment

$$\sigma_f^2 = \langle j_z^2 \rangle \frac{(A_p - A_f)(\nu A_p + A_f)}{(\nu + 1)^2(A_p - 1)}. \quad (2)$$

In Eq. (2),  $\langle j_z^2 \rangle$  is the average square of the spin projection,  $A_p$ ,  $A_f$  are masses of projectile and final fragment and  $\nu$  is the mean number of ablated nucleons per abrasion. Calculations for different  $\nu$  parameters have been performed.

Figure 4 shows the graphical comparison between experimental values determined in this work [13] and theoretical ones calculated for  $\nu = 0.5$  as used in the previous study [3]. In general, positive and negative parity isomers are — with few exceptions — well-described by this model and the  $R_{\text{exp}}/R_{\text{theor}}$  value is close to unity. For core-excited isomers,  $R_{\text{exp}}$  determined

in this work is better described by increasing  $\nu$  up to 1.0. Another group of isomers shown in Fig. 4 are isomers which have a spin lower than the ground state  $J_{gs}$ . The corresponding theoretical isomeric ratios are overestimated by orders of magnitude which is due to the assumption the SCM is based on. Integrating from  $J_m$  to infinity in Eq. (1) includes  $J_{gs}$  (because  $J_m < J_{gs}$ ) and is equivalent to a population of the isomer by decaying through the ground state which is not the case.

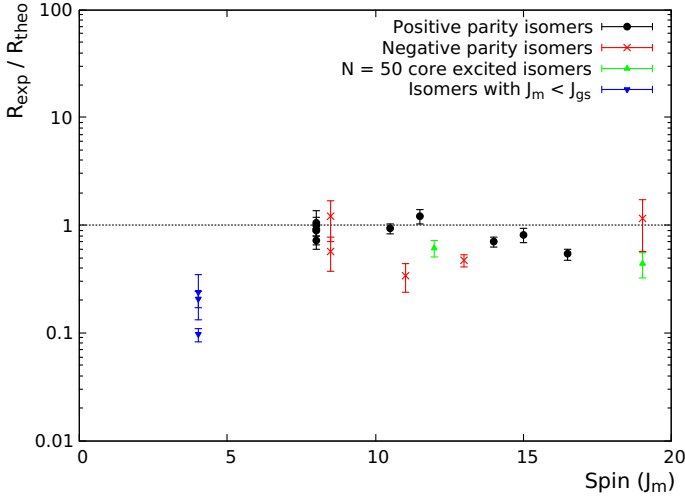


Fig. 4. Ratio of  $R_{\text{exp}}/R_{\text{theor}}$  plotted as a function of isomeric spin. The theoretical values correspond to calculations in the SCM employing  $\nu = 0.5$ . Different types of isomers are labelled accordingly.

## 5. Summary

In summary, half-lives and isomeric ratios of  $\gamma$ -decaying isomers around  $^{100}\text{Sn}$  were measured. The results for the half-life measurements are consistent with literature and the obtained isomeric ratios show large agreement with previous results. The preliminary results confirm the two recently discovered low-energy transitions of 55 keV in  $^{92}\text{Rh}$  and 44 keV in  $^{96}\text{Ag}$  and will be published elsewhere [13]. SM calculations of reduced transition probabilities were carried out in the  $\pi\nu(p_{1/2}g_{9/2})$  model space reproducing most of the new experimental  $B(\sigma\lambda)$  estimations.  $R_{\text{exp}}$  values were compared to theoretical calculations with the SCM and yield consistent results for most isomeric states. Large deviations are explained by the assumptions on which the model is based and expose its limitations.

This work was carried out at the RIBF operated by the RIKEN Nishina Center, RIKEN and CNS, University of Tokyo. The authors acknowledge the EUROBALL Owners Committee for the loan of germanium detectors and the PreSpec Collaboration for the readout electronics of cluster detectors. This work was partly supported by the German BMBF under contract No. 05P12PKFNE and No. 05P15PKFNA and by the U.S. DOE under grant No. DE-FG02-91ER-40609. G.H. is supported by the Bonn–Cologne Graduate School of Physics and Astronomy.

## REFERENCES

- [1] R.K. Wallace, S.E. Woosley, *Astrophys. J. Suppl.* **45**, 389 (1981).
- [2] T. Faestermann, M. Górska, H. Grawe, *Prog. Part. Nucl. Phys.* **69**, 85 (2013).
- [3] J. Park *et al.*, *Phys. Rev. C* **96**, 044311 (2017).
- [4] P.-A. Söderström *et al.*, *Nucl. Instrum. Methods Phys. Res. B* **317**, 649 (2013).
- [5] K. Moschner *et al.*, *EPJ Web Conf.* **93**, 01024 (2015).
- [6] K. Moschner, Ph.D. Thesis, Universität zu Köln, 2016.
- [7] P.J. Davies *et al.*, *Phys. Lett. B* **767**, 474 (2017).
- [8] T. Kubo *et al.*, *Prog. Theor. Exp. Phys.* **2012**, 03C003 (2012).
- [9] N. Warr, A. Blazhev, K. Moschner, *EPJ Web Conf.* **93**, 07008 (2015).
- [10] C.B. Hinke *et al.*, *Nature* **486**, 341 (2012).
- [11] M. Pfützner *et al.*, *Phys. Rev. C* **65**, 064604 (2002).
- [12] M.D. Bowry, Ph.D. Thesis, University of Surrey, 2013.
- [13] G. Haefner *et al.*, to be published.
- [14] G. Audi *et al.*, *Chin. Phys. C* **41**, 030001 (2017).
- [15] B.A. Brown, W.D.M. Rae, *Nucl. Data Sheets* **120**, 115 (2014).
- [16] M. de Jong, A.V. Ignatyuk, K.-H. Schmidt, *Nucl. Phys. A* **613**, 435 (1997).
- [17] J.-J. Gaimand, K.-H. Schmidt, *Nucl. Phys. A* **531**, 709 (1997).